A climatological-dynamical analysis associated with precipitation around the southern part of the Himalayas

B. C. Bhatt and K. Nakamura

Hydrospheric Atmospheric Research Center, Nagoya University, Nagoya, Japan

Received 9 May 2005; revised 19 October 2005; accepted 14 November 2005; published 31 January 2006.

[1] The precipitation variability and circulation characteristics around the Himalayas are examined using the Tropical Rainfall Measuring Mission (TRMM) data, the Global Energy and Water Cycle Experiment (GEWEX) Asian Monsoon Experiment (GAME) reanalysis, National Centers for Environmental Prediction–National Center for Atmospheric Research (NCEP-NCAR) reanalysis, and some of the Indian radiosonde data sets. The observation by precipitation radar on board the TRMM satellite reveals an afternoon maximum of precipitation during the premonsoon season and midnight–early morning maximum during the summer monsoon season over the southern slopes of the Himalayas. The data also shows that the morning precipitation moves southward in the mature monsoon season. The GAME reanalysis reveals a robust diurnal cycle of the atmospheric system that is coherent with the diurnal cycle of precipitation around the southern slopes of the Himalayas. The significant increase of moisture due to the southeasterly wind in the mature monsoon season seems to produce favorable conditions for the midnight–early morning rain. The down-valley wind at midnight probably triggers moist convection. The radiative cooling at the top of clouds may enhance the convection. The precipitation associated with the moist convection seems to generate a cold pool, which results in a density current. The downslope movement of the density current probably induces the southward movement of the precipitation system in the morning.

Citation: Bhatt, B. C., and K. Nakamura (2006), A climatological-dynamical analysis associated with precipitation around the southern part of the Himalayas, *J. Geophys. Res.*, *111*, D02115, doi:10.1029/2005JD006197.

1. Introduction

[2] A number of researchers have described the large-scale effects of the Himalayas and the Tibetan Plateau on the Asian summer monsoon [e.g., *He et al.*, 1987; *Chen et al.*, 1985] and continental-scale diurnal circulation in the monsoon region [e.g., *Krishnamurti and Kishtawal*, 2000]. These studies show that convection in the Himalayas and Tibetan Plateau plays an important role in sustaining the monsoon through the release of latent heat. Within many such studies, few have explicitly focused on the southern slopes of the Himalayas where vigorous interactions among climate, geomorphology and hydrology take place [*Burbank et al.*, 2003]. A general lack of systematic studies in hydrometeorology is due to the remoteness of the region, and the lack of meteorological data.

[3] Some studies of precipitation [e.g., *Barros and Lang*, 2003] have emphasized the deficiency of high-resolution precipitation data around the Himalayas. Because of the scarcity of rainfall data over the Himalayas, passive sensor data have been used as rainfall proxies to study the diurnal cycle. *Murakami* [1983] used Japanese Geostationary Meteorological Satellite data to examine the phase and amplitude of diurnal convection activity in the summer monsoon season. He noted heavy convection in the early morning hours and suppressed convection in the afternoon hours over the eastern Himalayan foothills. *Barros et al.* [2004] used infrared satellite data from Meteosat-5 to determine the small-scale spatial and temporal variations in the diurnal cycle of precipitation. They found that a diurnal cycle over the Himalayas was evident only over the southern slopes of the Himalayas with a peak at night (0000–0300 LT) during the summer monsoon season.

[4] Our investigation is related to a previous in situ observational study by *Barros and Lang* [2003] and a satellite-based precipitation study by *Bhatt and Nakamura* [2005]. *Barros and Lang* [2003] investigated summer monsoon precipitation characteristics, focusing on the onset phase, using rain gauge/radiosonde data over the central Nepal Himalayas. They identified a postmidnight peak in rainfall during June 2001, attributed to enhanced convection as a result of the interaction of ambient monsoon flows with the southern slopes, modulated by diurnal variation in atmospheric state. It was a basin-scale study that provided useful insight into the precipitation-generating processes. An interesting question is whether this mechanism would hold over the southern slopes of the Himalayas that constitute complex orography. *Lang and Barros* [2002] focused their attention particularly on the summer monsoon onset phase. They suggested a role of moist synoptic-scale low-

0148-0227/06/2005JD006197$09.00

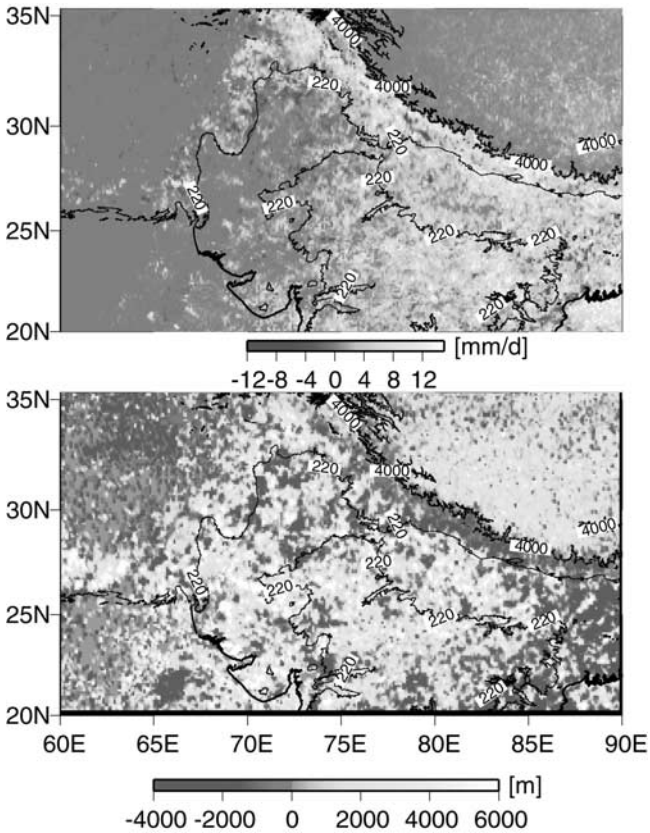

Figure 1. Horizontal distribution of rain amount difference between JJA near-surface mean daily total rainfall and MAM (upper panel). The lower panel shows similar seasonal difference (JJA-MAM) as the upper panel but for actual peak storm height. The topographic contours are also shown.

level flow in enhancing convection due to an influx of low-level moisture and the rising of conditionally unstable air along the southern slopes of the Himalayas.

[5] On the basis of the Tropical Rainfall Measuring Mission (TRMM) Precipitation Radar (PR) data, *Bhatt and Nakamura* [2005] noticed a strong diurnal cycle of moderate to heavy precipitation over the southern slopes of the Himalayas during the summer monsoon season. In addition to this, they reported that precipitation broadens and moves during midnight to early morning over the southern slopes of the Himalayas. *Bhatt and Nakamura* [2005] suggested the role of meridional circulation in the lower troposphere in triggering convection over the southern slopes of the Himalayas. However, they did not shed light on the circulation characteristics and thermodynamic environment in this region.

[6] The Himalayan mountains is characterized by a steep slope, which serves as an obstacle to flow. The intensity and spatial distribution of precipitation over a mountainous area depends on the synoptic-scale weather system over the region, on local air flow deviation and vertical motion and on microphysical processes that take place in clouds [*Wratt et al.*, 2000]. Because of the complex orography of the Himalayas, changes in flow at all levels, orographic gravity waves and daytime heating and nighttime cooling all can be influential factors in precipitation system generation [*Lang and Barros*, 2002].

[7] The paucity of observations made understanding of the circulation features over the Himalayas difficult. However, the advent of reanalysis data from many operational weather forecasting centers around the world has provided better understanding. There have been a few observational studies over the Himalayas as described earlier. At present, neither fine details of precipitation variations (e.g., spatial and temporal) are known nor is there a consensus on processes controlling the diurnal cycle of precipitation. The daytime heating, nighttime cooling of the Himalayan atmosphere, upscale convective organization and cooling by evaporation could be the key for the diurnal cycle of rainfall over the southern slopes of the Himalayas. *Barros and Lang* [2003] suggested mountain-forced gravity waves over the Himalayas. These mountain-forced gravity waves are expected to occur over the variable topography of the Himalayas. These waves may further enhance convection and subsequent precipitation. However, the influence of mountain breezes in triggering midnight–early morning precipitation cannot be neglected in this region. Development and propagation of the density current along the slope may influence southward migration of precipitation during the midnight to early morning in the summer monsoon season.

[8] The purpose of this study is to diagnose the low-level atmospheric systems surrounding the Himalayas. We adopt here a strategy of objective and subjective analysis to understand the atmospheric systems that contribute to precipitation. The paper is arranged in the following manner: Section 2 gives a description of data and method, section 3 gives the results and a discussion, and section 4 is the conclusion from the results.

2. Data and Method

[9] This study uses the following data sets: (1) The Global Energy and Water Cycle Experiment (GEWEX) Asian Monsoon Experiment (GAME) Intensive Observation Period reanalysis data with a spatial resolution of $0.5^\circ \times 0.5^\circ$, and a temporal resolution of 6 hours for the period from April to September in 1998. These data were extracted from ftp://hydro.iis.u-tokyo.ac.jp. (2) The National Centers for Environmental Prediction–National Center for Atmospheric Research (NCEP-NCAR) reanalysis (ftp://cdc.noaa.gov/cdc) with a spatial resolution of $2.5^\circ \times 2.5^\circ$, and a temporal resolution of 6 hours for JJA of the 5-year period 1998–2002. (3) Some of the Indian radiosonde data (http://raob.fsl.noaa.gov). These data were available for each meteorological season for the 5-year period 1998–2002. (4) Rain gauge data over the Nepal Himalayas for the period from April to September in 1998 from ftp://hydro.iis.u-tokyo.ac.jp. (5) The TRMM products 2A25, 2A23 and 2A12 (http://trmm.gsfc.nasa.gov). From 2A25, we accumulated and binned "near-surface rainfall rate" to hourly local times for the grid size of $0.05^\circ \times 0.05^\circ$ for each meteorological season for the 5-year period 1998–2002. We adopted a similar procedure for the radar reflectivity factor data set. The PR storm height data from 2A23 were accumulated and binned to hourly local times for $0.1^\circ \times 0.1^\circ$ for March–April–May (MAM) and June–

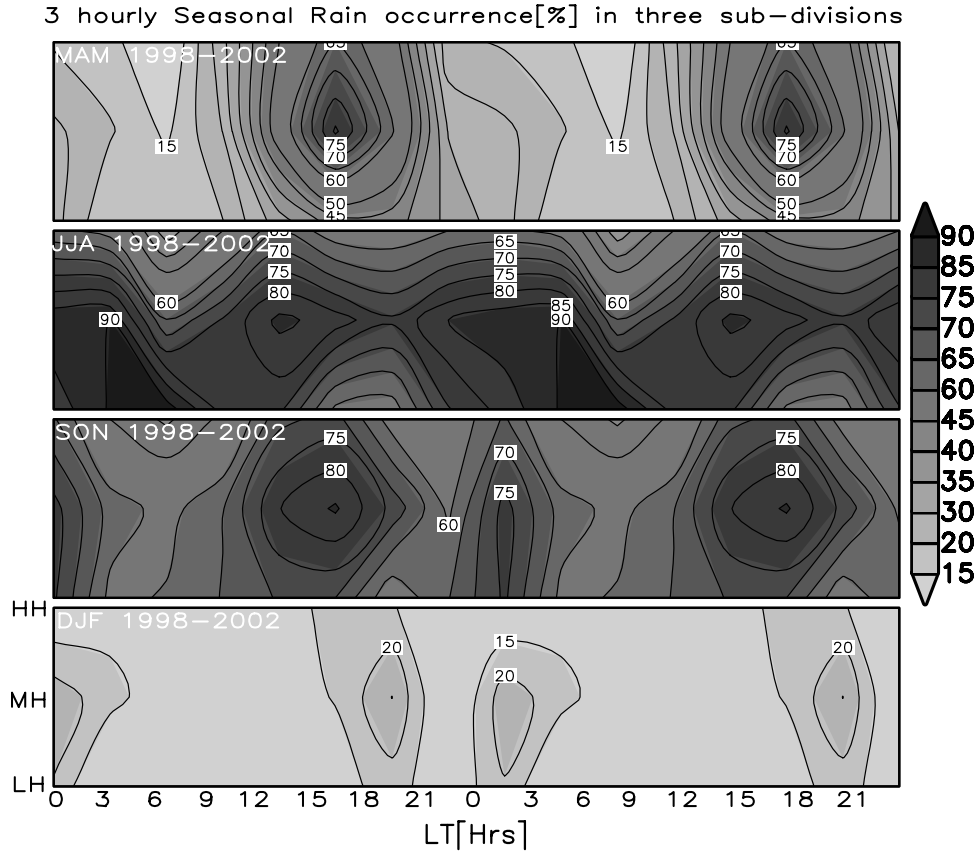

Figure 2. Areal representation of the seasonal variation of the diurnal cycle of rainfall occurrence in three climatic divisions over the Himalayas for eight time periods of a day. The LH, MH, and HH on the *y* axis stand for the lower, middle, and high Himalayas, respectively. See text for explanation.

July–August (JJA) of the 6-year period 1998–2003. In addition, the TRMM Microwave Imager (TMI) hourly total rainfall data with a spatial resolution of $0.2^\circ \times 0.2^\circ$ for JJA of the 6-year period 1998–2003 were utilized. The convective available potential energy (CAPE) data were extracted from a web site (http://weather.uwyo.edu/upperair). We mostly make use of climatological means.

3. Results and Discussion

3.1. Diurnal Variation of Precipitation

3.1.1. Horizontal Distribution

[10] To begin, we will examine spatial and temporal variation of precipitation around the Himalayas using PR data over 5 years (1998–2002) for four seasons. A difference of mean daily total rainfall between JJA (June–July–August) and MAM (March–April–May) is shown in Figure 1 (upper panel). This difference between two seasons shows higher precipitation amount over the Thar Desert and east coast of India in MAM. The premonsoon circulation around the Hindkus-Himalayas is characterized by a low-level westerly/southwesterly flow regime. Larger rain totals appear over the northern Indian subcontinent and southern slopes of the Himalayas in the summer monsoon season. The summer monsoon activity around the Himalayas is associated with the development and westward propagation of monsoon depressions originating from the Bay of Bengal [e.g., *Lang and Barros*, 2002]. These inferences are similar to those given by *Bhatt and Nakamura* [2005]. Note that there is a decrease of peak (maximum) storm height over the southern slopes of the Himalayas, and an increase over the northern Indian subcontinent and the Tibetan Plateau in the summer monsoon season (lower panel, Figure 1). Actual storm height used in our analysis is the top of the precipitation column above the ground level instead of the mean sea level. These results suggest that the storms are somewhat shallow over the southern slopes of the Himalayas as compared to other regions in the summer monsoon season. The diurnal cycle of horizontal distributions of near-surface rainfall was plotted around the Himalayas for each meteorological season. These figures (not shown) suggested pronounced diurnal variation with afternoon maximum for MAM over the southern slopes of the Himalayas. Some studies [e.g., *Minoura et al.*, 2003] linked this maximum to strong boundary layer heating. Other seasons that exhibited daytime maximums were September–October–November (SON) and December–January–February (DJF). As a unique feature, midnight–early morning maximum and its southward progression were noticed during JJA over southern slopes of the Himalayas (refer to *Bhatt and Nakamura* [2005] for more details). We also noticed similar features in area-averaged rainfall occurrence over the three climatic divisions of the Himalayas (Figure 2). The southernmost climatic division, lower Himalayas (LH) span from approximately 200 to 500 m MSL. The middle Himalayas (MH)

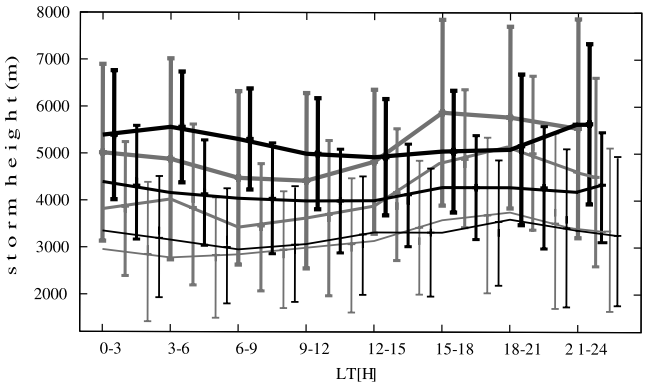

Figure 3. Areal representation of the seasonal variation of the diurnal cycle of actual mean storm height over three climatic divisions with standard deviation plotted (shown by error bars). The solid gray and black lines represent MAM and JJA, respectively. The bold solid, medium bold solid, and thin solid lines represent LH, MH, and HH, respectively.

rise from 500 m to 2000 m MSL succeeding the LH. The high Himalayas (HH) rise to 8848 m MSL succeeding the MH. These climatic divisions (77°–90°E; run nearly SE-NW with approximately a 60-km width (north-south)) roughly correspond with the geometry of the Himalayas. We counted rainfall occurrence over each climatic division. These plots show normalized percentage of rainy grids during 3-hour intervals in each climatic division.

[11] The TMI observation around the Himalayas is not a focus of this study, but it is nevertheless interesting to analyze diurnal cycle of precipitation, realizing the benefit of its wider swath. Here, we try to confirm the spatial variability in the diurnal cycle using TMI data set. We produced mean 3-hourly horizontal distributions of total rainfall using fine resolution data (not shown) during the summer monsoon season. The midnight–early morning peak of rainfall and its southward progression also appeared in TMI observations.

[12] There is considerable spatial and temporal variability in the rainfall distribution around the Himalayas. We next present area-averaged 3-hourly diurnal cycle of mean storm height in three climatic divisions over the Himalayas (Figure 3). There is an increase of storm height during MAM at 1500–1800 LT. The storms appear relatively higher in the lower Himalayas at 0300–0600 LT during JJA. Note that there is less spatial variability of storm height with a relatively smaller standard deviation in the summer monsoon season as compared to the premonsoon season.

3.1.2. Vertical Distribution

[13] A different perspective of precipitation can be shown by making use of vertical structure of radar reflectivity factor. As anticipated from our earlier discussion on horizontal variability, the vertical profiles of radar reflectivity factor could show relatively similar geographical variability over the Himalayas. We selected radar reflectivity factor above the noise level. By selecting these data above the terrain, we gridded for $0.05^\circ \times 0.05^\circ$ over three climatic divisions of the Himalayas (refer to *Bhatt and Nakamura* [2005] for area description). Figure 4 shows the climatological diurnal cycle of the radar reflectivity factor and its vertical distribution averaged over the 82.5°–85.0°E longitudinal belt during JJA. To give an idea of the variability of upward motion over this region, the area-averaged mean vertical velocity in the lower and middle troposphere from GAME reanalysis is plotted (white dashed contour). Although mean vertical velocity is small, it hints of a relatively stronger upward motion. Description of GAME reanalysis will be presented later. There appears daytime northward progression of precipitation denoted by "A" and midnight–early morning southward denoted by "B." The PR reveals trailing stratiform precipitation in this region. There is a relatively deep but small precipitation system in the foothills of the Himalayas at 0300–0600 LT. Minimum rain activity appears at 0600–0900 LT. At the extreme high elevations, daytime precipitation cells are enhanced as denoted by "C." This tendency strongly supports the notion of up-valley flow being responsible for daytime precipitation in the high elevations [*Barros and Lang*, 2003]. These averaged radar reflectivities do not exceed 35 dBZ and are situated at or below the brightband altitude of approximately 5.5 km MSL. Reflectivities in excess of 25 dBZ rarely extend up to 8 km. We also studied the climatological diurnal cycle of the radar reflectivity factor for MAM of the 6-year period 1998–2003 over the same longitudinal belt (82.5°–85.0°E). We found that the averaged radar reflectivities did not exceed 42 dBZ (not shown). The vertical profiles depicted isolated deeper precipitation cells than in the summer monsoon season with no brightband. *Barros et al.* [2004] noted maximum lightning flashes over the Himalayas during May of 1999. Hence it is anticipated that premonsoon precipitation cells can develop vertically deep with lightning. We did not notice the midnight–early morning peak of precipitation and its southward migration. Although the vertical structure of precipitation cells smaller than the PR footprint may not be well represented, this view of precipitation was not available before TRMM PR. Overall, the analysis of precipitation does confirm substantial diurnal and seasonal variability in this region.

3.2. Circulation and Thermodynamic Diagnostics

[14] Here we examine the climatological context of the atmospheric system. The GAME has provided reanalyzed fields covering the atmospheric system for the period, March–October 1998. These data may be the best choice as they were assimilated from intensive observations around the Himalayas. We mostly used climatological variables (e.g., wind, moisture, temperature) from GAME reanalysis, which are available at 6 hour intervals with a $0.5^\circ \times 0.5^\circ$ grid for 17 atmospheric levels. On the basis of the availability of data, the 6-month period was divided into two seasons: a premonsoon season for April and May, and a summer monsoon season from June to September. A good representation of mesoscale convective system cannot be expected using these data sets because of the complex terrain in this region. Since the data period is not long enough to obtain a climatological mean value, we make use of NCEP-NCAR reanalysis and some of the Indian radiosonde data.

3.2.1. Horizontal Structure

[15] We first investigated circulation characteristics around the Himalayas. Figure 5 shows area-averaged upper

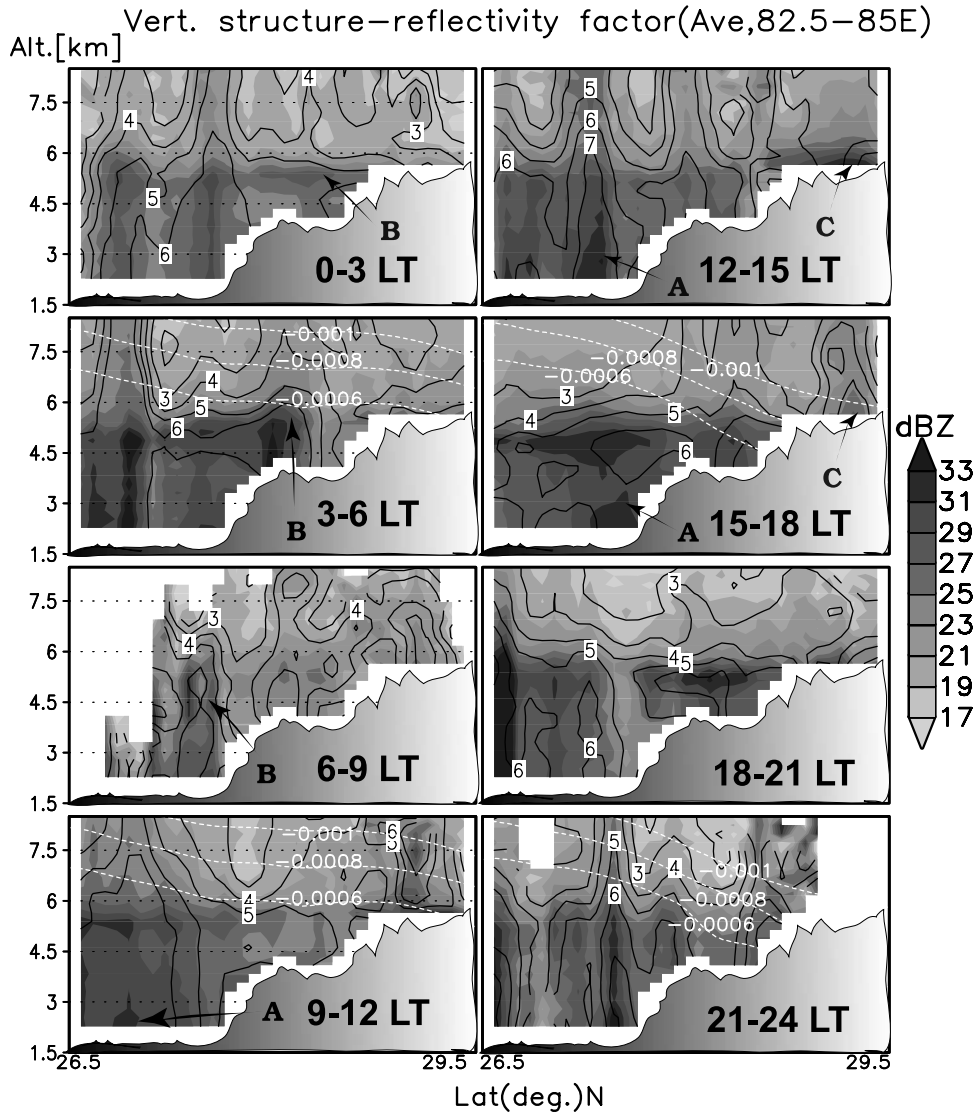

Figure 4. Diurnal variation of the vertical profiles of radar reflectivity factor averaged over 82.5°–85.0°E longitudinal belt from PR during JJA of 1998–2003. The solid contours represent standard deviation, label by label for each 250 km by 5 km segment from south to north. The white dashed contours represent climatological mean vertical velocity (m s^{-1}) averaged over the 80°–85°E longitudinal belt from GAME reanalysis. For further explanation, refer to text.

tropospheric zonal wind (U) for region (77°–87°E, 25°–31°N) and lower tropospheric temperature advection for the region (77°–87°E, 25°–27.5°N) from GAME reanalysis. The sign convention is nonstandard, with negative U being westerly flow (Figure 5a). The winds switch to westerlies at the monsoon onset and these prevail throughout the summer monsoon season, which is in agreement with many other studies [e.g., *Barros and Lang*, 2003; *Krishnamurti and Kishtawal*, 2000] in this region. The diurnal cycle of zonal wind seems weak. However, afternoon winds appear relatively stronger. *Krishnamurti and Kishtawal* [2000] also reported similar characteristics of zonal wind and proposed a hypothesis that linked intensification of zonal wind to radiative forcings, such as the heating and cooling of the Tibetan Plateau. The temperature advection is the negative of the dot product of the wind vector and the gradient of temperature. In most of the days, there appears warm air advection (Figure 5b). The premonsoon warm air advection is weaker as compared to the summer monsoon season. This is because of the relatively weak near-surface winds during premonsoon. *Lang and Barros* [2002] characterized the Himalayan region as a region of positive advection of temperature and moisture during the monsoon onset. A feature worthy of noting is the stronger diurnal cycle during the summer monsoon onset with relatively stronger warm air advection at midnight to early morning. These tendencies suggest the existence of rising air on a synoptic scale.

[16] We next focus on the common fields (e.g., air temperature, relative humidity) in the lower troposphere over the central Himalayas. The area-averaged (81°–85°E, 25.5°–27.5°N) air temperature shows a stronger diurnal cycle in the premonsoon season (Figure 6a). This is probably related with the weak cloud cover. The analysis at 925 hPa depicts the weak diurnal variation of relative

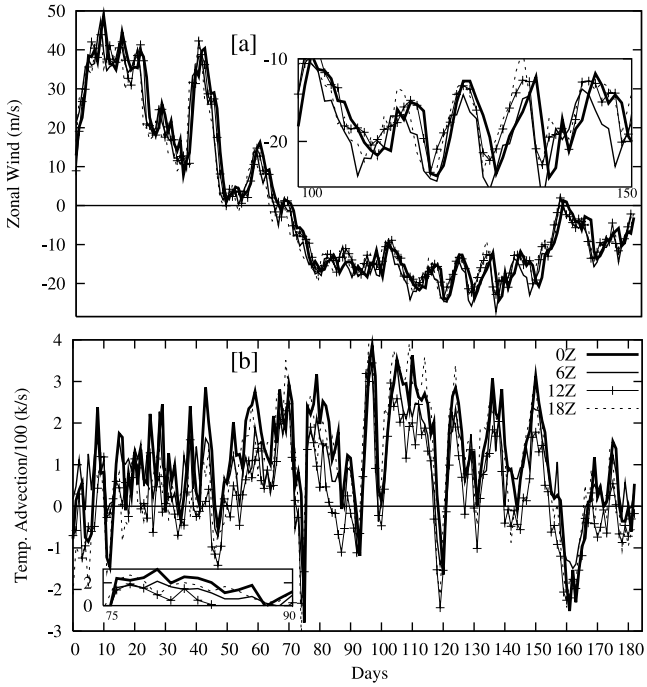

Figure 5. Area-averaged (a) upper tropospheric zonal wind at 200 hPa and (b) lower tropospheric temperature advection at 925 hPa from GAME reanalysis for 1 April to 30 September 1998. The inserts show a few days' evolution with an expanded scale in the monsoon period. For further explanation, refer to text.

humidity in the premonsoon season (Figure 6b). The premonsoon southwesterly winds impinging the Himalayas are from the arid regions. Consequently, the air is hot and dry. In this context, predominant afternoon peak of rainfall over southern slopes could be linked to the local moisture source. *Weston* [1972] showed cumulonimbus convection over the eastern foothills of the Himalayas in the premonsoon season. *Minoura et al.* [2003] suggested high OLR in premonsoon over northern India. They postulated that the inland region between 20°N and 25°N remains warmer during 16–22 April and 30 April to 6 May. Our results suggest that there is nighttime high relative humidity and cooling of the air temperature in the summer monsoon season. From a thermodynamic perspective, this combination is good for precipitation development. These inferences are similar to those given by *Barros and Lang* [2003]. Despite the fact that the GAME reanalysis variables are available only four times per day, the GAME reanalysis captures the diurnal cycle.

[17] The Himalayan range is located nearly in the meridional wall and provides a huge barrier to the flow of weather systems, tending to block the flow and cause convergence. The summer monsoon circulation pattern is markedly different from that of the premonsoon season over the Himalayas. There is a strong, moist low-level southeasterly wind from the wet regions in the summer monsoon season. The moisture flux is the product of wind vector and specific humidity, which is often used to investigate precipitation potential. Moreover, the wind governs the transport and distribution of moisture. Examination of the diurnal cycle of moisture flux in the lower atmosphere over the Himalayas reveals a weak moisture transport in premonsoon (Figure 7a). This suggests weak near-surface winds during premonsoon. The low-level moisture influx from the Bay of Bengal has obvious importance for the summer monsoon precipitation in this region. During the summer monsoon season there is maximization of moisture flux in the midnight–early morning hours (Figure 7b). This is related to nighttime strengthening of wind. During the summer monsoon season, we noticed a relatively stronger, low-level horizontal wind at nighttime (not shown). There was well-defined cyclonic tendency during midnight–early morning in the vicinity of the Himalayas. Note that the cyclonic tendency was similar to that appears in these moisture flux horizontal distributions. There is considerable weakening of cyclonic pattern at 0600 UTC (1200 LT). When mesoscale depressions originating from the Bay of Bengal interact with easterly vertical shear forced by the Himalayan mountains, strong near-surface flow and weaker flow in the midlevel establishes cyclonic circulation [*Lang and Barros*, 2002]. There is strong moisture convergence very close to, but not on, the southern slopes of the Himalayas at 1800 UTC (0000 LT). This convergence line does not coincide precisely with the position of enhanced precipitation at midnight. This discrepancy is probably due to the poor spatial and temporal resolution of GAME reanalysis.

3.2.2. Vertical Structure

[18] Here we focus on the vertical structure of the premonsoon and the summer monsoon circulation to understand three-dimensional flows. The premonsoon and

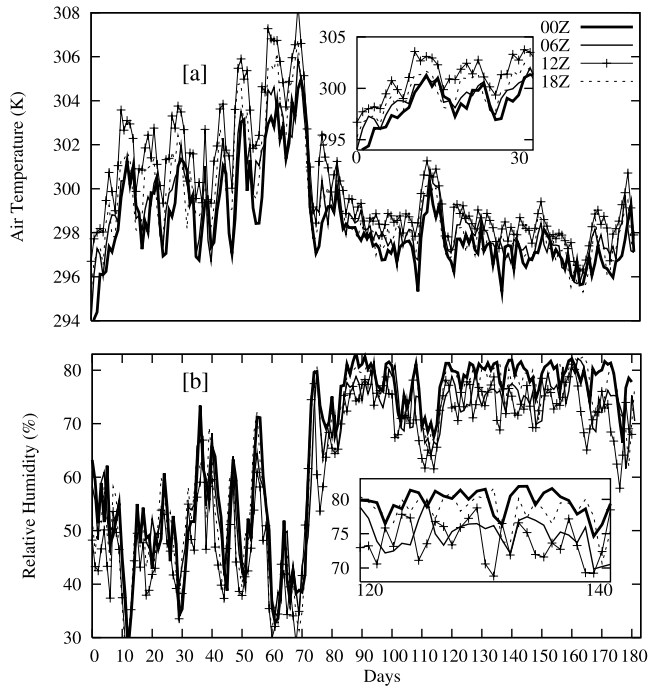

Figure 6. Area-averaged lower tropospheric (a) air temperature at 925 hPa and (b) relative humidity at 925 hPa from the GAME reanalysis for 1 April to 30 September 1998. The inserts show a few days' evolution with an expanded scale. See text for explanation.

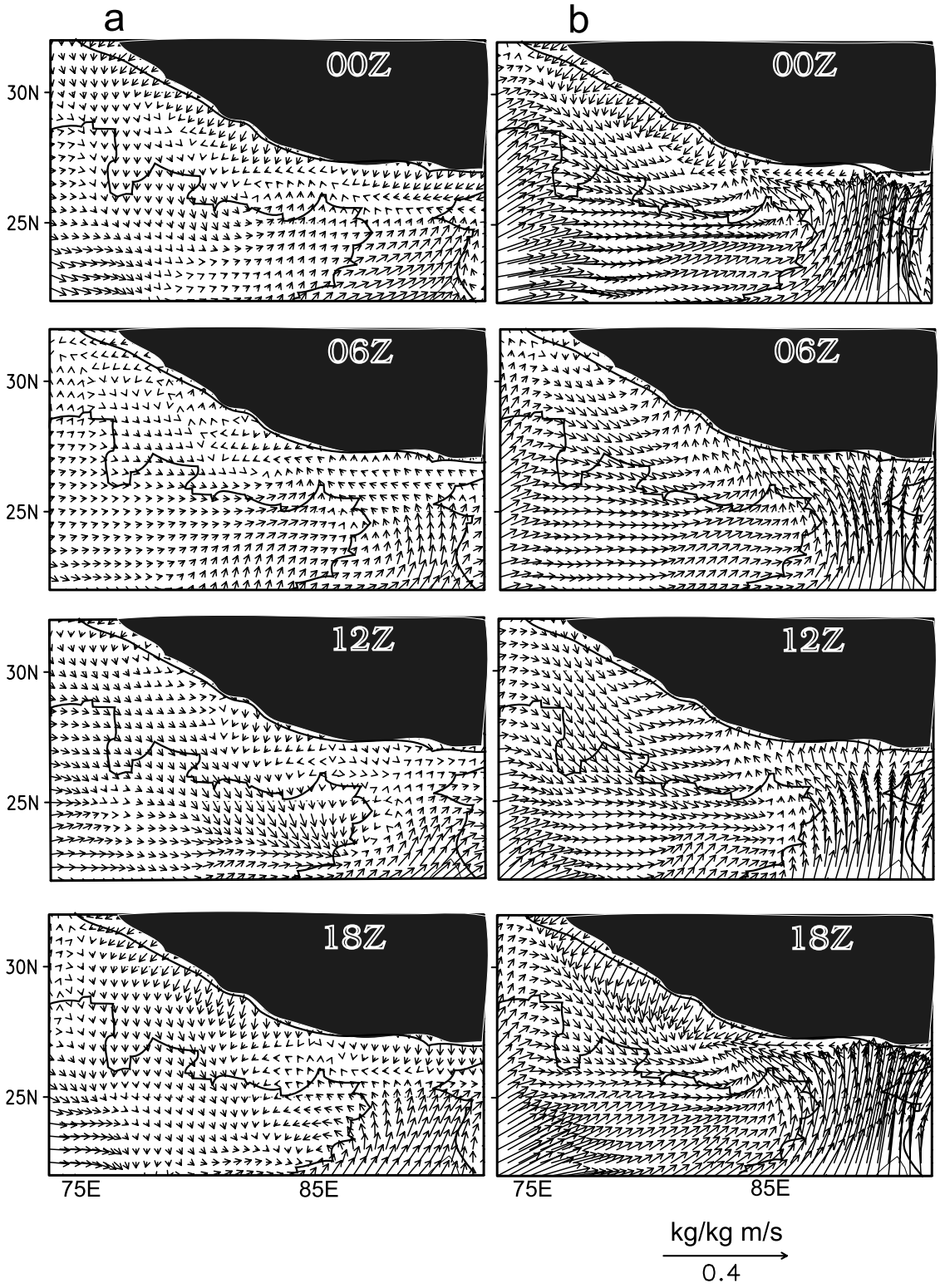

Figure 7. Diurnal cycle of the climatological mean moisture flux at 925 hPa from the GAME reanalysis for indicated time periods during (a) April–May and (b) June–July–August–September. Also shown are smoothed-out 500 m topographic contours.

summer monsoon climatological vertical structure of the circulation field from GAME reanalysis are shown in Figures 8a and 8b. During premonsoon, there is weak meridional wind and upward motion near to the Himalayas in the lower atmosphere. There appears a weak moisture convergence at 0000 UTC (0600 LT) that is a fairly shallow feature centered roughly in foothills (Figure 8a). This is probably related with the morning position of dry line over northern India during the premonsoon season [*Weston*, 1972]. Midnight–early morning moisture conver-

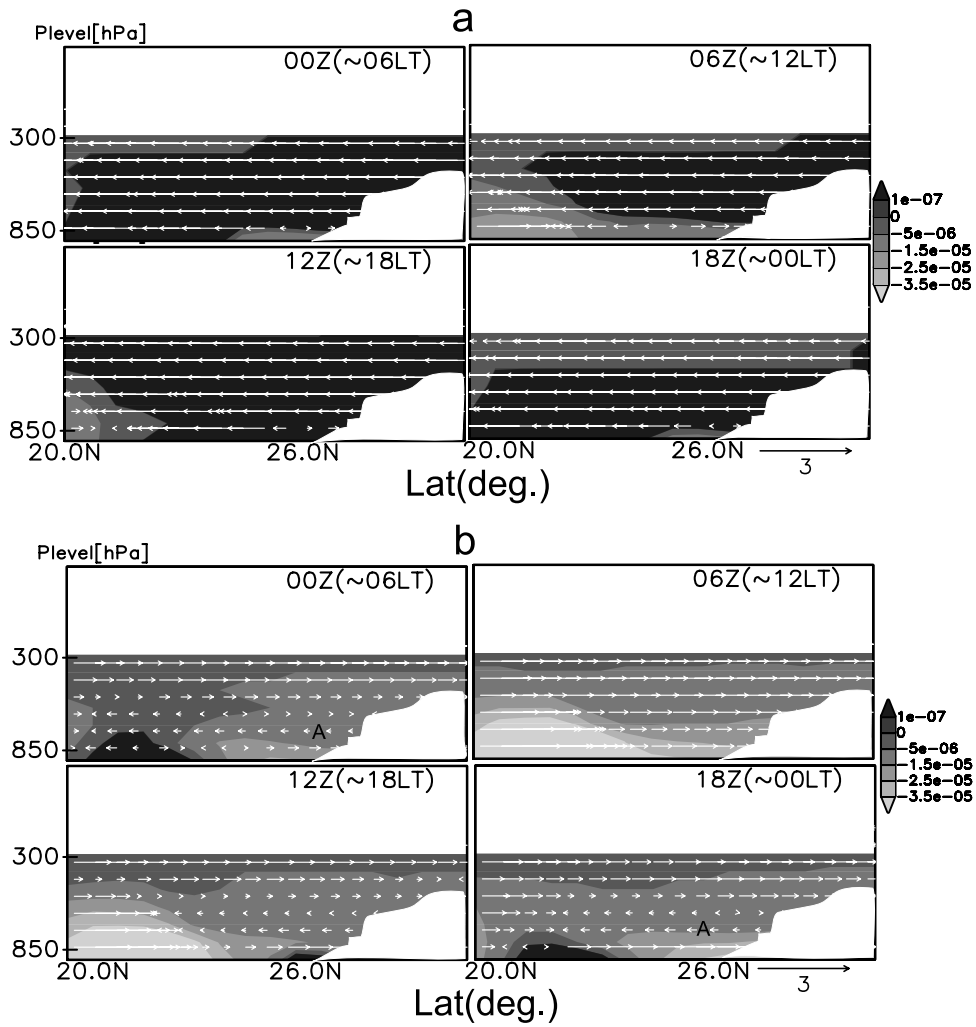

Figure 8. Height-latitude sections of climatological mean meridional wind component and vertical velocity (v and vv (m s^{-1})) below 300 hPa averaged for 80°–85°E for indicated time periods during (a) April–May and (b) June–September. Also shown is moisture flux divergence (g kg^{-1} s^{-1}), with shading with negative sign being convergence.

gence is noticed in the lower atmosphere in the vicinity of southern slopes of the Himalayas in the summer monsoon season (Figure 8b). There is also a weak midlevel return flow denoted by "A" during nighttime (1800 UTC and 0000 UTC), which seems absent at 0600 UTC (1200 LT). Over the Indian subcontinent, moisture convergence appears during the daytime.

[19] *Chater and Sturman* [1998] postulated that convective activity due to orographic lifting is an important process in the generation of rainfall over mountains. The difference in equivalent potential temperature with height (for layer 700–925 hPa) was used to estimate the existence and strength of convective instability (CI). The six-month-long evolution averaged over the 75°–80°E longitudinal belt using the GAME reanalysis suggested weak CI in the premonsoon season over the region (not shown). During summer monsoon, the CI was relatively higher as compared to premonsoon. We did not notice solid evidence from reanalysis data for a diurnal cycle of CI. *Minoura et al.* [2003] noted enhanced CI around the eastern coast of India during premonsoon. Though they focused over the eastern coast of India, some of their results reveal low-level moisture flux convergence over the Himalayas after the commencement of the summer monsoon. All of these tendencies are conducive to convection and precipitation over the southern slopes of the Himalayas. The GAME reanalysis suggests a robust diurnal cycle of the atmospheric system, which is coherent with the precipitation diurnal cycle in the mature monsoon period. The significant increase of the moisture due to the southeasterly wind in the mature monsoon season seems to produce favorable conditions for precipitation system generation. We further hypothesize that there may be a favorable environment for the generation of orographically induced gravity waves over the southern slopes of the Himalayas. The gravity wave activity is often associated with topography and has a link to atmospheric convection [*Koch and O'Handly*, 1997].

3.3. Gravity Wave Environment

[20] There are four or five radiosonde stations in India that are relatively close to the Himalayas. However, sound-

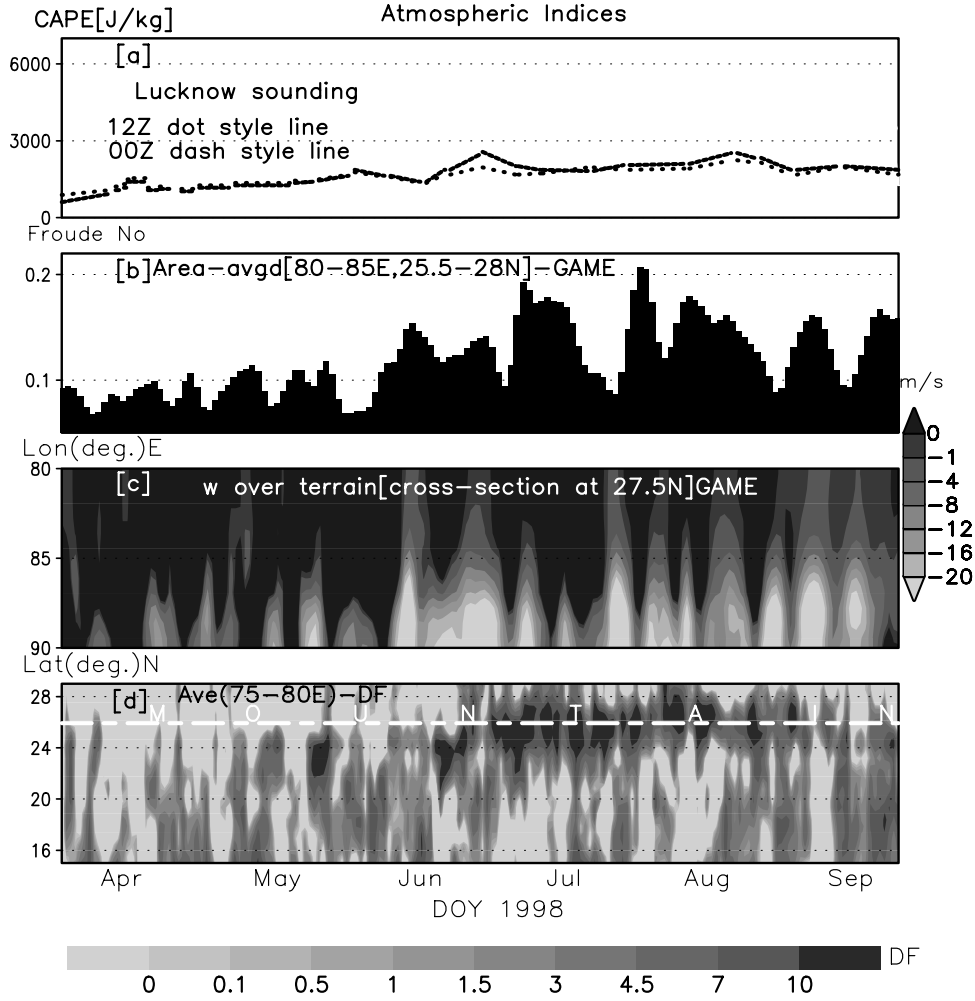

Figure 9. Six-month-long evolution of atmospheric indices. Figure 9a represents the daily variation of smoothed-out convective available potential energy from the Lucknow radiosonde. Figures 9b and 9c represent mean daily area-averaged Froude number and cross section of vertical velocity induced by flow over terrain using 850 hPa wind field, respectively. The time-latitude variations of mean daily duct factor (DF) averaged over the 75°–80°E longitudinal belt are shown in Figure 9d.

ings from these regions are somewhat flawed [*Collins*, 1992]. Moreover, the low frequency of sounding flights (at best 2 per day; 0000 and 1200 UTC) precludes the ability to determine the diurnal cycle of atmospheric system. Despite this, quality controlled data sets provide a basic understanding on atmosphere close to the Himalayas. The convective available potential energy (CAPE) is considered as a measure of atmospheric instability [*Moncrieff and Miller*, 1976] or an indicator of the likely occurrence of deep convection. Some of the studies [e.g., *Barros and Lang*, 2003] suggested synergistic interaction between atmospheric instability and gravity waves, and here our interest lies in investigating gravity wave environment over the southern slopes of the Himalayas. Further descriptions of sounding station parameters and indices (e.g., CAPE) for Indian radiosonde can be found at http://weather.uwyo.edu/upperair/indices.html. The smoothed-out six-month-long evolution of CAPE for the period from April to September in 1998 was plotted. The Patna radiosonde (not shown) showed a relatively higher CAPE at 1200 UTC (1800 LT) while the Delhi and Patiyala soundings (not shown) showed no such difference in CAPE between the 0000 (0600) and 1200 UTC (1800 LT). However, the 0000 UTC (0600 LT) CAPE is slightly higher than the 1200 UTC (1800 LT) CAPE during the summer monsoon season from the Lucknow radiosonde located at 80.88°E, 27.5°N (shown in Figure 9a). *Barros and Lang* [2003] also noticed maximum CAPE at midnight to early morning during the onset of the summer monsoon at Besisahar station in the Himalayas of central Nepal. The Indian soundings should be viewed skeptically, and the more trust should be placed in the Besisahar sounding, as it possesses high temporal resolution and quality control.

[21] To access the potential for blocking to occur, crude estimates of Froude number (*Fr*) were calculated for the Himalayas of central Nepal, taking Θ at 850 hPa and 600 hPa with mountain height of approximately 3000 m using GAME reanalysis. It is evident that flow is blocked in both seasons (Figure 9b). There is relatively high *Fr* value in the summer monsoon season. This is because of stronger wind in spite of higher stability. This suggests that monsoon wind can flow over mountain ridges in the

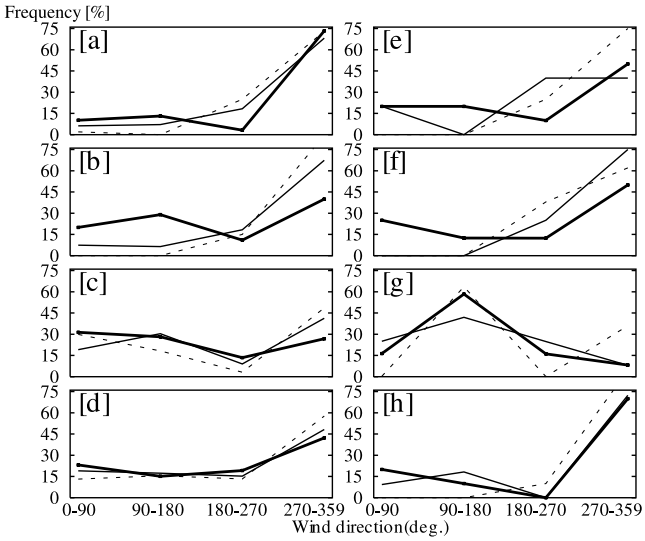

Figure 10. Diurnal and seasonal variation of frequency of the wind direction at Lucknow: 0000 UTC for (a) DJF 1998–2002, (b) MAM 1998–2002, (c) JJAS 1998–2002, and (d) ON 1998–2002 and 1200 UTC for (e) DJF 1998–2002, (f) MAM 1998–2002, (g) JJAS 1998–2002, and (h) ON 1998–2002. The bold solid, thin solid, and dotted lines represent frequency at 925 hPa, 850 hPa, and 700 hPa, respectively. See text for further explanation.

southern slopes of the Himalayas. In addition, even though the moist air may not be able to flow over the high Himalayas, the high *Fr* value may help moist air to be lifted sufficiently high along the southern slopes. Note how the crude estimate of vertical velocity ($w = u\delta h/\delta x + v\delta h/\delta y$) induced by flow over terrain (Figure 9c, cross section at 27.5°N) shows an example for favorable mountain geometry and a confluent flow field [*Lin et al.*, 2001]. The result suggests a potential for upward vertical motion in the presence of strong low-level flow over southern slopes of the Himalayas. More importantly, the summer monsoon season shows strong upward motion.

[22] The relatively high *Fr* value could help generating mountain-forced gravity waves. On the basis of *Koch and O'Handly* [1997], we computed six-month-long evolution of duct factor, taking into account potential temperature, Θ and equivalent potential temperature, Θ_e ($[DF = \Theta_{850} - \Theta_{925}] + [\Theta_{e850} - \Theta_{e400}]$) averaged over the 75°–80°E longitudinal belt using GAME reanalysis (Figure 9d). This gravity wave index is a measure of the favorable conditions for gravity wave generation. The southeasterly flow is not as strong, but it should be enough to force gravity waves over the Himalayas (refer to Figure 2 of *Barros et al.* [2004]). If there is a duct then vertically propagating gravity waves may be trapped with a concentration of wave energy in the horizontal direction leading to westward-northwestward propagation along the mountain. At least the summer monsoon shows positive high index value (greater than 10 K). While the mountain-forced gravity waves occur on a mesoscale, one must be cautious in the interpretation of these results, as coarse resolution of reanalysis mostly reveals synoptic-scale features. The relatively high *Fr* value and high duct index suggests more active gravity waves in the summer monsoon. The exact link of atmospheric instability and vertical motion associated with gravity waves or wave ducting to the evolving precipitation patterns over the Himalayas remains to be investigated.

3.4. Low-Level Cold Air Advection

[23] The southward diurnal movement in the summer monsoon season is another feature of the precipitation over the southern slopes of the Himalayas. We hypothesize that the movement is due to the density current. To investigate the cause of southward diurnal progression of precipitation during midnight–early morning in the summer monsoon season, we make use of NCEP-NCAR reanalysis and the Indian radiosonde data for the period of 1998–2002. More description of quality controlled radiosonde data set can be found at http://raob.fsl.noaa.gov/. We utilized the wind field from the Lucknow radiosonde. Although the height resolution of the data was quite coarse, we noticed good height resolution data at near surface in very few instances. Because of our interest in investigating the linkages between the density current and the wind field, we will focus our discussion on the lower troposphere. Seasonal variation of relative frequency of wind directions is shown in Figure 10. The frequency refers to the total wind field at a given height represented by flow from a particular direction. We counted occurrence at 90° angle bin to produce histogram. Westerly winds seems to be most frequent during DJF, with a slight reduction in frequency during October–November (ON) and MAM. The June–July–August–September (JJAS) winds are very different. The frequency of near-surface winds from north-northeast

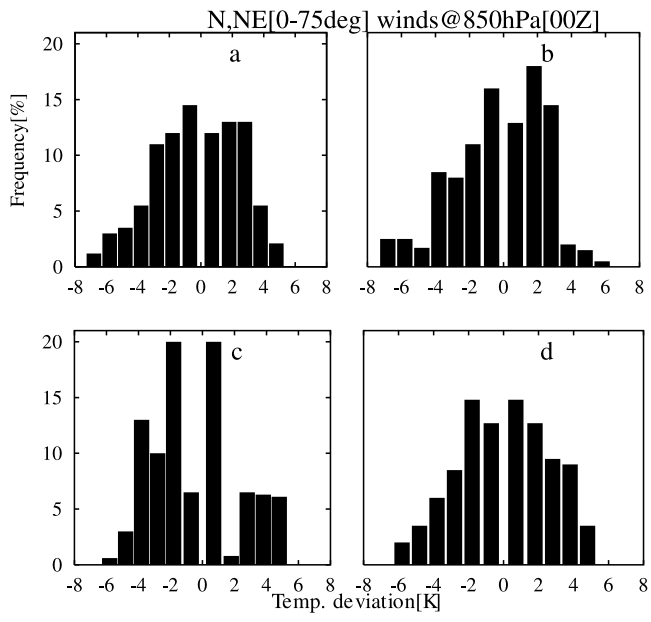

Figure 11. Histograms of temperature deviation at 0000 UTC for N, NE (0°–75°) wind from NCEP-NCAR reanalysis during June–July–August–September of 1998–2002. Figures 11a, 11b, 11c, and 11d represent 77.5°E, 30°N; 80°E, 27.5°N; 82.5°E, 27.5°N; and 85°E, 27.5°N positions of 2.5° × 2.5° Himalayan grids, respectively.

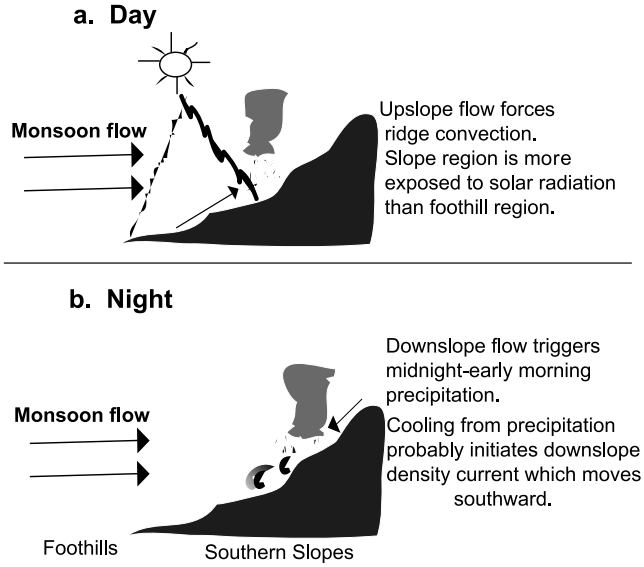

Figure 12. (a and b) Schematic illustration of the mechanism to explain rainfall over the southern slopes in the summer monsoon season.

appears to be definitive during JJAS (0000 UTC), which is presumed to be the result of cold air advection from the mountains. On the contrary, southerly flow is dominant at 1200 UTC (1800 LT). One thing to be noted is that number of soundings at 1200 UTC (1800 LT) did not exceed 20 in any season. However, there were ten times more soundings at 0000 UTC (0600 LT).

[24] We further investigated early morning temperature fields with the help of NCEP-NCAR reanalysis during JJAS of 1998–2002. The frequency distributions of the temperature deviation from the seasonal averages at 850 hPa are shown in Figure 11 for north-northeasterly (0–75°) wind. From reanalysis data, the frequency was calculated as a ratio of days that belong to the respective interval divided by the number of all days with north-northeasterly wind for the Himalayan region grids. This is a temperature deviation for all north-northeasterly days in JJAS. It is anticipated that early morning north-northeasterly winds bring cooler temperatures from the Himalayan mountains, which could relate to the density current. Analysis of histograms shows that north-northeasterly winds bring cooler weather because of the relatively large number of negative deviations. *Keevallik et al.* [1999] related circulation types and temperature in Estonia using a similar technique. *Lang and Barros* [2002] also noticed low-level cold air advection near to the mountain barrier during the onset of the summer monsoon season. *Barros and Lang* [2003] suggested the increasing trend in the down-valley wind at nocturnal hours was due to cool outflow from rainstorms over the central Nepal Himalayas. This suggests evaporation cooling in this region. The motion of the density current is difficult to determine by existing data sets but appears to be approximately 10.4 m s^{-1}, if we simply relate such a current to near-surface precipitation. Precipitation shifts approximately 300 km in an approximately 8 hours interval (refer to *Bhatt and Nakamura* [2005] for 3-hourly PR images). This speed is reasonably consistent with the density current speed [*Sun et al.*, 2002]. This suggests a robust atmospheric system and supports the notion of density current. However, clearer description of the phenomenon is limited because of the scarcity of data in this region. Further observational work is required to understand the exact mechanism of the density current.

3.5. Dynamical Interpretation

[25] The mechanism we presented here (Figure 12) suggests a robust atmospheric system that is behind the Himalayan rainfall variability in the summer monsoon season. Ambient monsoon flow is presumed to be roughly constant during day and night. Earlier, *Bhatt and Nakamura* [2005] advocated similar situation using NCEP-NCAR reanalysis meridional wind field. During daytime, the southern slopes are presumed to be more exposed to solar radiation than the foothills, though the frequency of cloudy days is high over the Himalayas in the summer monsoon season. After sunrise, precipitable water vapor increases over the mountain slope because of surface evaporation as a result of solar radiation. Some two-dimensional numerical studies [e.g., *Sato and Kimura*, 2003] discussed the diurnal cycle of precipitation over a mountain slope. Besides the ambient wind direction, various aspects of up-valley wind in their research can be considered similar to those over southern slopes of the Himalayas. At low elevations, there could be weakening of spatial gradients of wind due to the interaction between the up-valley flow and large-scale flow. The thermally induced up-valley winds help ridge convection. The observed afternoon peak of precipitation supports this assumption.

[26] At night, the spatial gradient of wind does not weaken because of the decline of daytime turbulence (up-valley flow). Hence there is nighttime strengthening of wind leading to increase in influx of moisture. *Sato and Kimura* [2003] discussed the importance of ambient wind for water vapor transport over a lee of mountain. On the other hand, the atmosphere above the mountain starts to cool down. The near coincidence of these processes lead to release of low-level convective instability. Such atmospheric conditions are favorable for precipitation generation. The observed precipitation around midnight over the southern slopes of the Himalayas supports this hypothesis. The widespread cloud systems that suppress the diurnal variation of the surface temperature could have the same characteristics as over ocean where morning maximum of precipitation occurs. The heating and cooling of the surface of the very high mountain may be another important mechanism to enhance the midnight–early morning precipitation. Even though clouds cover wide area frequently in the summer monsoon season, the high mountain region could be less frequently covered by clouds. Thus the heating and cooling may be significant there. The nighttime cooling at the high mountain region probably enhances the down-valley wind. The cloud top cooling may also play an important role. The collision of the up-valley wind by general monsoon flow and the down-valley wind likely forces precipitation systems.

[27] Once the rainfall activity has begun over the higher elevations, these areas begin to cool because of precipitation. The cool outflow from rainstorms increases the down-valley tendency of wind at low levels over the central Nepal

Himalayas [*Barros and Lang*, 2003]. Similar characteristics were reported by *Steiner et al.* [2003] in the Alps. It can be argued that density current is induced by the cooling due to evaporation of the precipitating particles over the southern slopes of the Himalayas in the summer monsoon season. Our proposed mechanism explains why this density current is most likely in the summer monsoon season only. In the summer monsoon season, there are frequent precipitation systems over the southern slopes of the Himalayas due to very moist air inflow. The hypothesis of evaporational cooling appears to be in agreement with the downward decrease in vertical profiles of radar reflectivity factor below the melting level in this region as suggested by *Hirose and Nakamura* [2002].

[28] Some of the atmospheric indices provide an impression that gravity waves are most likely over the Himalayas in the summer monsoon season. Hence gravity waves may also prompt the release of low-level convective instability in the regions of forced ascent. *Reinking et al.* [2000] showed that orographically produced gravity waves can have important effects on rainfall. We speculate that these processes could be more active in the favorable thermodynamics in the midnight–early morning hours. The cooling of land surface at night is most likely in the premonsoon season due the absence of clouds. However, the mean monthly land surface temperature in cloud-free environment derived from the Moderate Resolution Imaging Spectroradiometer (MODIS) on the Terra and Aqua platforms (http://earthobservatory.nasa.gov/observatory/Datasets/) also showed relatively cooler surface at night over the Himalayan range in the mature monsoon period (not shown). These factors help to enhance the duct index.

4. Conclusions

[29] This study focused on precipitation as well as on the lower atmospheric system around the Himalayas. An intercomparison was made between states during premonsoon and the summer monsoon periods. There is increase of peak (maximum) storm height over the southern slopes of the Himalayas, and decrease over the northern Indian subcontinent and the Tibetan Plateau during MAM. An inspection of the diurnal cycle of precipitation appeared in PR observations reveals an afternoon maximum during the premonsoon season and midnight–early morning maximum during the summer monsoon season over the southern slopes of the Himalayas. The diurnal signal is relatively stronger at low levels. However, vertical distribution of precipitation does not differ significantly up to 4–5 km height. The GAME reanalysis reveals a robust diurnal cycle of the atmospheric system that is coherent with precipitation diurnal cycle during the premonsoon and the summer monsoon season around the southern slopes of the Himalayas. In the summer monsoon season, wide cloud cover due to the moist air induced by the low-level southeasterly wind suppresses the diurnal variation of surface temperature. The down-valley wind may still occur because of much less cloud cover over the high mountain region. The significant increase of the moisture due to the southeasterly wind in the mature monsoon season seems to produce favorable conditions for precipitation system generation. The collision of the up-valley wind by general monsoon flow and the down-valley wind likely forces precipitation systems in the midnight–early morning. The cloud top radiative cooling may also enhance the moist convection.

[30] The precipitation associated with the moist convection seems to generate a cold pool, which results in a density current. The downslope movement of the density current induces the southward movement of the precipitation system in the morning. A clear description of the density current phenomenon is inadequate because of the scarcity of data in this region.

[31] Our crude estimation of indices reveal favorable conditions for gravity wave occurrence over the Himalayas. The gravity waves may prompt the release of low-level convective instability and enhance convection and precipitation. We speculate that these processes could be more active in the favorable thermodynamics at midnight–early morning. In recent months, numerical simulation of orographic gravity waves over the central Nepal Himalayas has been conducted (A. P. Barros, Duke University, personal communication, 2004). So far, there is no observational evidence for gravity waves over the Himalayas. The results give interesting indications, but further field measurements are needed to understand the exact mechanism of Himalayan rainfall.

[32] **Acknowledgments.** The authors would like to express gratitude to members of the TRMM and GAME projects as well as to members of the laboratory of satellite meteorology of the Hydrospheric Atmospheric Research Center. Helpful comments in this research offered by M. K. Yamamoto, A. Higuchi, M. Hirose, and A. P. Barros are appreciated. R. Swindell and J. Lamsal kindly checked the manuscript. The constructive criticisms of anonymous reviewers greatly improved this manuscript. This work was supported by the TRMM project in the Japan Aerospace Exploration Agency.

References

Barros, A. P., and T. Lang (2003), Monitoring the monsoon in the Himalayas: Observations in central Nepal, June 2001, *Mon. Weather Rev.*, *131*, 1408–1427.

Barros, A. P., G. Kim, E. Williams, and S. W. Nesbitt (2004), Probing orographic controls in the Himalayas during the monsoon using satellite imagery, *Nat. Hazards Earth Syst. Sci.*, *4*, 29–51.

Bhatt, B. C., and K. Nakamura (2005), Characteristics of monsoon rainfall around the Himalayas revealed by TRMM precipitation radar, *Mon. Weather Rev.*, *133*, 149–165.

Burbank, D. W., A. E. Blythe, J. Putkonen, B. Pratt, E. Gabet, M. Oskin, A. Barros, and T. P. Ojha (2003), Decoupling of erosion and precipitation in the Himalayas, *Nature*, *426*, 652–655.

Chater, A. M., and A. P. Sturman (1998), Atmospheric conditions influencing the spillover of rainfall to lee of the southern Alps, New Zealand, *Int. J. Climatol.*, *18*, 77–92.

Chen, L., E. R. Reiter, and Z. Feng (1985), The atmospheric heat source over the Tibetan Plateau: May–August 1979, *Mon. Weather Rev.*, *113*, 1771–1790.

Collins, W. G. (1992), The operational complex quality control of radiosonde heights and temperatures at the National Centers for Enviornmental Prediction. Part II: Examples of error diagnosis and correction from operational use, *J. Appl. Meteorol.*, *40*, 152–168.

He, H., J. W. McGinnis, Z. Song, and M. Yanai (1987), Onset of the Asian monsoon in 1979 and the effect of the Tibetan Plateau, *Mon. Weather Rev.*, *115*, 1966–1995.

Hirose, M., and K. Nakamura (2002), Spatial and seasonal variation of rain profiles over Asia observed by speceborne precipitation radar, *J. Clim.*, *15*, 3443–3458.

Keevallik, S., P. Post, and J. Tuulik (1999), European circulation patterns and meteorological situation in Estonia, *Theor. Appl. Climatol.*, *63*, 117–127.

Koch, S., and C. O'Handly (1997), Operational forecasting and detection of mesoscale gravity waves, *Weather Forecasting*, *12*, 253–281.

Krishnamurti, T. N., and C. M. Kishtawal (2000), A pronounced continental-scale diurnal mode of the Asian summer monsoon, *Mon. Weather Rev.*, *128*, 462–473.

Lang, T. J., and A. P. Barros (2002), An investigation of the onsets of the 1999 and 2000 monsoons in central Nepal, *Mon. Weather Rev.*, *130*, 1299–1316.

Lin, Y. L., S. Chiao, T. Wang, M. L. Kaplan, and R. P. Weglarz (2001), Some common ingredients for heavy orographic rainfall, *Weather Forecasting*, *16*, 633–660.

Minoura, D., R. Kawamura, and T. Matsuura (2003), A mechanism of the onset of the south Asian summer monsoon, *J. Meteorol. Soc. Jpn.*, *81*, 563–580.

Moncrieff, M. W., and M. J. Miller (1976), The dynamics and simulation of tropical cumulonimbus and squall lines, *Q. J. R. Meteorol. Soc.*, *102*, 373–394.

Murakami, M. (1983), Analysis of the deep convective activity over the western Pacific and Southeast Asia. Part I: Diurnal variation, *J. Meteorol. Soc. Jpn.*, *61*, 60–77.

Reinking, R. F., J. B. Snider, and J. L. Coen (2000), Influences of storm-embedded orographic gravity waves on cloud liquid water and precipitation, *J. Appl. Meteorol.*, *39*, 733–759.

Sato, T., and F. Kimura (2003), A two-dimensional numerical study on diurnal cycle of mountain lee precipitation, *J. Atmos. Sci.*, *60*, 1992–2003.

Steiner, M., O. Bousquet, R. A. Houze Jr., B. F. Smull, and M. Mancini (2003), Airflow within major alpine river valleys under heavy rainfall, *Q. J. R. Meteorol. Soc.*, *129*, 411–432.

Sun, J., et al. (2002), Intermittent turbulence associated with a density current passage in the stable boundary layer, *Boundary Layer Meteorol.*, *105*, 119–219.

Weston, K. J. (1972), The dry-line of northern India and its role in cumulonimbus convection, *Q. J. R. Meteorol. Soc.*, *98*, 519–531.

Wratt, D. S., M. J. Revell, M. R. Sinclair, W. R. Gray, R. D. Henderson, and A. M. Chater (2000), Relationships between air mass properties and mesoscale rainfall in New Zealand's Southern Alps, *Atmos. Res.*, *52*, 261–282.

B. C. Bhatt and K. Nakamura, Hydrospheric Atmospheric Research Center, Nagoya University, Furocho, Chikusa-ku, Nagoya 464-8601, Japan. (bhatt@satellite.hyarc.nagoya-u.ac.jp)